Catalysis Today 156 (2010) 93–99

Contents lists available at ScienceDirect

Catalysis Today

journal homepage: www.elsevier.com/locate/cattod

A multifunctional Pd/alumina hollow fibre membrane reactor for propane dehydrogenation

Ejiro Gbenedio, Zhentao Wu, Irfan Hatim, Benjamin F.K. Kingsbury, K. Li*

Department of Chemical Engineering and Chemical Technology, Imperial College London, London SW7 2AZ, UK

ARTICLE INFO

Article history:
Available online 15 June 2010

Keywords:
Alumina hollow fibre
Asymmetric structure
Pd membrane
SBA-15
Membrane reactor
Dehydrogenation of propane

ABSTRACT

Following a successful development of a hollow fibre membrane reactor (HFMR-I) [1], a highly compact multifunctional Pd/alumina hollow fibre membrane reactor (HFMR-II) was further developed and applied to the catalytic dehydrogenation of propane to propene. The developed HFMR-II consists of a thin and defect-free Pd membrane coated directly onto the outer surface of an alumina hollow fibre substrate with a unique asymmetric pore structure, i.e. a sponge-like outer layer and a finger-like inner layer where Pt (1 wt.%)/SBA-15 catalyst is deposited. Benefiting from this novel design, the functionalized alumina hollow fibre substrates with a surface area/volume value of up to 1918.4 m^2/m^3 possess a catalyst surface area of 31.8 m^2/g, which is significantly higher than that of the HFMR-I in which Pt (0.5 wt.%)/γ-Al_2O_3 catalyst is deposited. In contrast with a conventional fixed bed reactor (FBR), greater propene selectivity and a one order of magnitude higher space-time yield (STY) have been achieved by using the HFMR-II for propane dehydrogenation. Although the process controlling step in the HFMR-II is believed to be the catalytic reaction, as a consequence of catalyst deactivation due to coke-formation, the advantages of HFMR-II, such as easy catalyst deposition and high catalytic surface area for catalytic reactions, are promising for other catalytic reactions with less coking problems, such as the water–gas-shift (WGS) reaction and steam reforming (SR) etc.

1. Introduction

In the last several decades, inorganic catalytic membrane reactors (CMR) combining catalytic reaction and separation into a single unit have attracted extensive attention in the research community [2–5] and can be divided into two major categories of dense CMRs in view of the function of the membranes. The first is the use of a membrane to selectively remove a product from a reaction that is limited by chemical equilibrium [6,7], shifting the reaction towards the product side and simplifying subsequent product separations. The second is the use of a membrane to simultaneously purify and uniformly distribute a reactant throughout the reactor [8,9], offering a high level of control over how the reactants interact.

Use of Pd or Pd-alloy membranes in CMR, where the membrane "extracts" hydrogen – a critically important energy carrier – from a reaction, has been proved experimentally and theoretically to be efficient in enhancing conversions and/or lowering operating temperatures of endothermic, equilibrium-limited reactions [4,7] such as the dehydrogenation of propane [10,11] ($C_3H_8 \leftrightarrow C_3H_6 + H_2$, $\Delta H^\circ = 124$ kJ/mol). Thin and defect-free Pd or Pd-alloy membranes with high hydrogen permeability and selectivity can be supported by porous alumina hollow fibres [12–20] with to date the highest surface area/volume value, demonstrating the advantages of using composite membranes of this type in hydrogen separation. Moreover, in one of our recent studies, porous alumina hollow fibres with a unique asymmetric pore structure [21], i.e. a sponge-like outer layer and a finger-like inner layer, have been developed by using a one step dry–wet spinning/sintering technique [12]. Such alumina hollow fibres have also been used for the construction of a highly compact hollow fibre membrane reactor (HFMR-I) for propane dehydrogenation by directly coating a thin Pd/Ag membrane onto the outer surface of the alumina hollow fibres and depositing Pt (0.5 wt.%)/γ-Al_2O_3 catalyst into the finger-like inner layer [1]. The deposition of sub-micron sized catalyst particles was repeated 3 times in order to obtain a reasonable loading of catalyst, offering an increase in the surface area of the reaction zone (5 cm in length) of up to about 0.22 m^2 in the HFMR-I made with a single hollow fibre.

In order to further improve the process of depositing catalyst into the asymmetric alumina hollow fibres and to achieve a higher surface area in the reaction zone, which can be critically important in improving the performance of CMR in catalytic reactions such as water–gas-shift (WGS) and steam reforming (SR) reactions, mesoporous silica (SBA-15) [22] with a surface area as high as about 850 m^2/g [23] and significant thermal stability up to 1473 K [24] has been prepared inside the finger-like structure of the asymmetric

* Corresponding author. Tel.: +44 0 207 5945676; fax: +44 0 207 5945629.
E-mail address: Kang.Li@Imperial.ac.uk (K. Li).

0920-5861/$ – see front matter © 2010 Elsevier B.V. All rights reserved.
doi:10.1016/j.cattod.2010.04.044

alumina hollow fibres in this study, by using an easy and efficient method via liquid-paraffin-medium protected solvent evaporation [25,26]. After impregnating Pt onto the deposited SBA-15 and coating a Pd hydrogen separation membrane onto the outer surface of the functionalized alumina hollow fibre substrates, a highly compact multifunctional HFMR-II with a surface area/volume ratio of up to about 1918.4 m^2/m^3 is developed. Greater propene selectivity as well as a one order of magnitude higher space-time yield (STY) has been achieved when compared with a conventional fixed bed reactor (FBR) for propane dehydrogenation. In contrast with HFMR-I, a significant increase in the surface area of HFMR-II is achieved by replacing γ-Al_2O_3 with mesoporous SBA-15. Although the performances of two HFMR designs are comparable as a consequence of catalyst deactivation in dehydrogenation of propane, the advantages of HFMR-II can be applied to other catalytic reactions of great importance, such as WGS and SR etc. with less catalyst deactivation problems.

2. Experimental

2.1. Materials

2.1.1. Alumina hollow fibres

Aluminium oxide powders of 1 μm (alpha, 99.9% metals basis, S.A. 6–8 m^2/g), 0.05 μm (gamma–alpha, 99.5% metals basis, S.A. 32–40 m^2/g) and 0.01 μm (gamma–alpha, 99.98% metals basis, S.A. 100 m^2/g) were purchased from Alfa Aesar and were used as supplied. Polyethersulfone (PESf, Radel A-300, Ameco Performance, USA), *N*-methyl-2-pyrrolidone (NMP, HPLC grade, Rathbone) and Arlacel P135 (Uniqema, UK) were used as binder, solvent and additive, respectively. DI water and tap water were used as the internal and external coagulants, respectively, for the fabrication of alumina hollow precursor fibres.

2.1.2. Electroless plating of Pd membrane

Pd $(NH_4)_2Cl_4$ (ammonium tetrachloropalladate, 99.99%, Aldrich), $SnCl_2{\cdot}2H_2O$, $Na_2EDTA{\cdot}2H_2O$, HCl (37%), N_2H_4 and $NH_3{\cdot}H_2O$ (28%) (Fisher Sci. Ltd.) were used for preparing the Pd hydrogen separation membrane.

2.1.3. Mesoporous silica SBA-15

Tetraethoxysiliane (TEOS) as a silica source and poly-(ethylene oxide)-poly(propylene oxide)-poly(ethylene oxide) (PEO-PPO-PEO) amphiphilic block copolymer $EO_{20}P_{O7}0EO_{20}$ (Pluronic P123, MW = 5800, Aldrich) as structure-directing agent were used for the preparation of mesoporous silica SBA-15. H_2PtCl_6 (99.995%, Aldrich) as a Pt source was used for preparing Pt (1 wt.%)/SBA-15 catalyst.

2.2. Fabrication of multifunctional HFMR-II

2.2.1. Asymmetric alumina hollow fibre substrates

Asymmetric alumina hollow fibre substrates were fabricated via a dry–wet spinning/sintering technique [12]. The preparation of the alumina spinning suspension has been described elsewhere [21]. The resultant spinning suspension was degassed under vacuum for 2 h to fully remove air bubbles trapped inside. After degassing, the suspension was transferred to a Harvard stainless steel syringe of 200 ml in volume and was extruded through a tube-in-orifice spinneret (ID = 1.2 mm, OD = 3.0 mm) into a coagulation bath containing 120 L of water with an air-gap of 15 cm. DI water was used as the internal coagulant and the flow rate ranged from 5 to 15 ml/min. The extrusion rate of the spinning suspension and the flow rate of the internal coagulant were accurately controlled and monitored by two individual Harvard PHD 22/2000 Hpsi syringe pumps, ensuring the uniformity of the prepared precursor fibres. The formed precursor fibres were first heated in a CARBOLITE tube furnace at 873 K for 2 h to remove the organic polymer binder and were then sintered at 1723 K for 4 h with heating and cooling rates of 5 K/min. The outer surfaces of the sintered substrates (about 30 cm in length) were coated with a thin and gas-tight glaze layer with the exception of the central part of the fibre of 5 cm in length, which was left unglazed for the subsequent electroless plating (ELP) of Pd membrane

2.2.2. Catalyst preparation and deposition

The synthesis of mesostructured silica monoliths, which were used as the support for the Pt catalyst, has been reported elsewhere [25]. For a typical synthesis, 5 g of P123 was first dissolved fully in a mixture consisting of 25 g of ethanol and 1 g of aqueous HCl (1 mol/L). 10.4 g of TEOS was then slowly added to the solution under stirring, forming a transparent sol. The unglazed outer surface of the alumina hollow fibre substrate was covered by a thin layer of epoxy resin and the fibres were immersed in the resultant sol and were degassed under vacuum for 1 h at room temperature, removing air trapped in the finger-like voids of the substrates and allowing the infiltration of the sol into the substrates. After degassing, the remaining sol in the substrate lumen was expelled using compressed air. The substrates were then placed in a flowing air stream at room temperature for 48 h, during which the sol in the substrates changed to gel. After that, the substrates were heated at 333 K for 20 h in liquid-paraffin and sintered at 823 K for 6 h with heating and cooling rates of 0.5 K/min, during which the gel changed into silica SBA-15 inside the finger-like voids of the substrate, while the thin epoxy resin layer on the outer surface of the substrate was simultaneously removed. The amount of deposited silica SBA-15 was determined by measuring the weight gain of the samples. Pt was subsequently impregnated onto the deposited silica SBA-15 by immersing the resultant samples in an aqueous solution of H_2PtCl_6 at room temperature. After impregnation, the substrates with the Pt (1 wt.%)/SBA-15 catalyst in the finger-like voids were dried at 383 K overnight and calcined at 773 K for 4 h with heating and cooling rates of 2 K/min

2.2.3. Pd membrane coating

The Pd membranes were coated directly onto the unglazed outer surface of the functionalized alumina hollow fibre substrates by a conventional ELP method [7]. Prior to coating, the substrates were cleaned and activated by the Pd–Sn activation procedure. The activation process consisted of successive immersion of the substrates in tin(II) chloride ($SnCl_2$) solution and palladium chloride ($PdCl_2$) solution at room temperature. Deionised water and 0.1 M HCl were used to rinse the samples between the immersions. The activation process was repeated 6 times, after which the substrate surface turned brown. The Pd membrane was coated using a plating bath having the composition as the one described elsewhere [27].

2.3. Characterizations of HFMR-II

The morphology of the asymmetric alumina hollow fibre substrates, the coated Pd membranes and the mesoporous silica SBA-15 deposited into the finger-like voids were visually observed using a scanning electron microscope (SEM, JEOL JSM-5610LV, Tokyo, Japan). The pore structures of the functionalized asymmetric alumina hollow fibre substrates were characterized by mercury intrusion porosimetry (Autopore IV 9500, Micromeritics) and BET. EDS analysis (INCA Energy by Oxford Instruments) was employed to investigate the elemental distribution across the cross-sections of the composite Pd/alumina hollow fibre membranes.

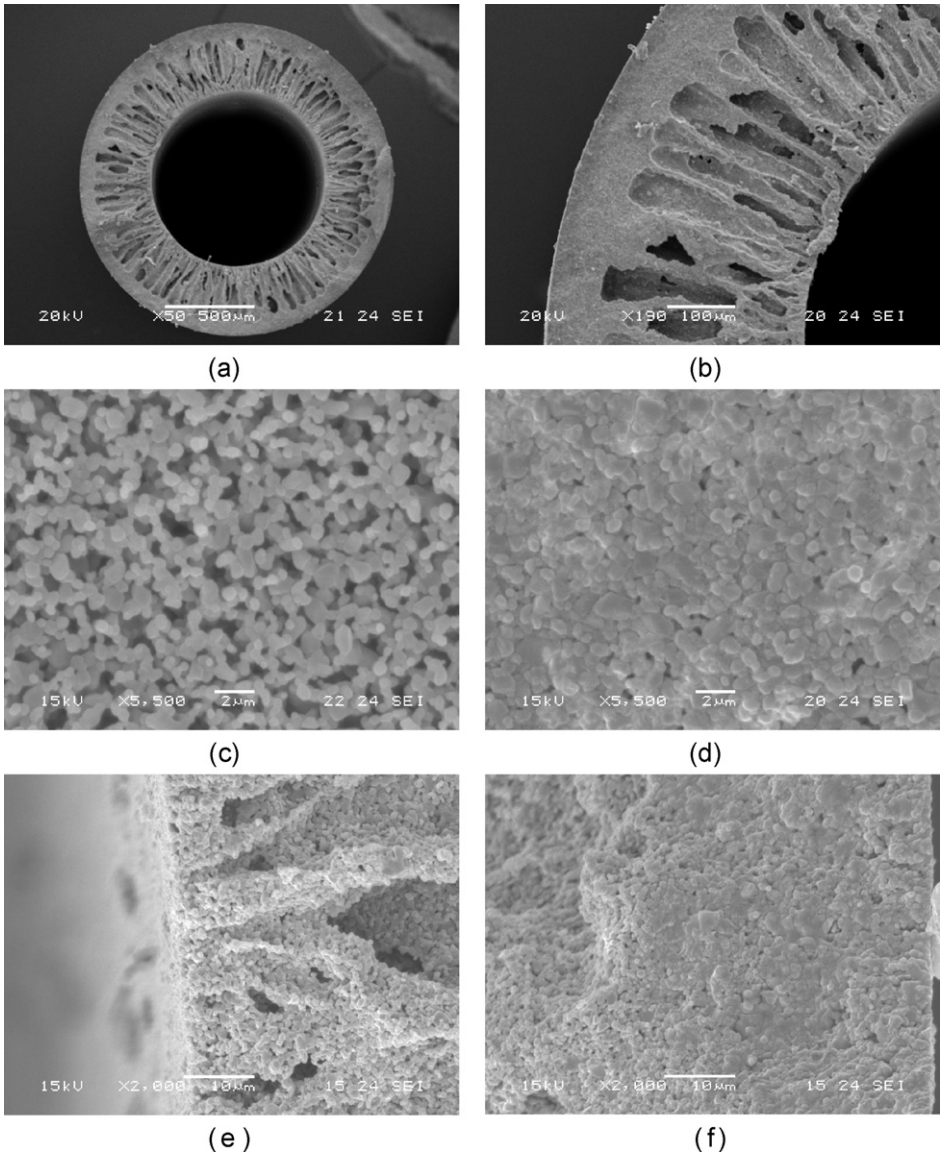

Fig. 1. SEM images of the asymmetric alumina hollow fibre substrate sintered at 1723 K for 4 h: (a) whole view, (b) cross-section, (c) inner surface, (d) outer surface, (e) inner edge and (f) outer edge.

2.4. Dehydrogenation of propane to propene using HFMR-II

The apparatus for dehydrogenation of propane to propene has been described elsewhere [1]. A gaseous stream containing propane (5 vol.%) and hydrogen (4.5 vol.%) with balanced nitrogen was introduced at 30 ml/min into the lumen of the reactor. Argon with a flow rate of 50 ml/min was used as a sweep gas to carry the permeated hydrogen to a TCD gas chromatograph (Varian-3900) for analysis. The membrane reactor was operated at atmospheric pressure and the effluent gases from the reactor were analyzed on-line using a FID gas chromatograph (Varian-3900).

3. Results and discussion

3.1. Microstructure of asymmetric alumina hollow fibre substrates

As a result of instabilities at the interface between the non-solvent (internal coagulant) and the spinning suspension [21], the prepared alumina hollow fibre substrates possess a unique asymmetric pore structure that is characterized by a thin, uniform sponge-like outer layer and a thick finger-like inner layer (Fig. 1a and b). Finger-like voids extend across approximately 80% of the fibre cross-section from a highly porous inner surface (Fig. 1c) with the remaining 20% consisting of the sponge-like outer layer, forming a smooth and denser outer surface (Fig. 1d). The entrances of the finger-like voids exist in a thin, highly porous inner skin-layer (Fig. 1e), while no finger-like structures are found in the sponge-like outer layer (Fig. 1f). The OD and ID of the sintered hollow fibre substrates with uniform wall thickness were measured at approximately 1893 μm and 964 μm, respectively, resulting in a surface area/volume value of up to 1918.4 m^2/m^3. It should be noted here that this value can be further increased to 2789.0 m^2/m^3 when porous YSZ hollow fibres (OD = 1300 μm) with similar asymmetric structures [28] are employed, yielding a significantly higher surface area per volume value for HFMR.

The asymmetric pore structures, especially those above 100 nm, of the sintered alumina hollow fibre substrates were then quantified by mercury intrusion porosimetry. As can be seen in Fig. 2, two distinct peaks, i.e. a narrow, strong peak at 6.03 μm and a wide, weak one at 151.4 nm are observed, indicating the mean

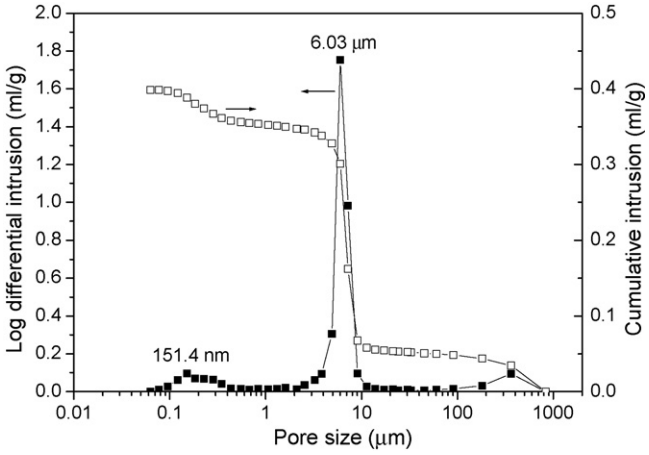

Fig. 2. Mercury intrusion of the asymmetric alumina hollow fibre substrates sintered at 1723 K for 4 h.

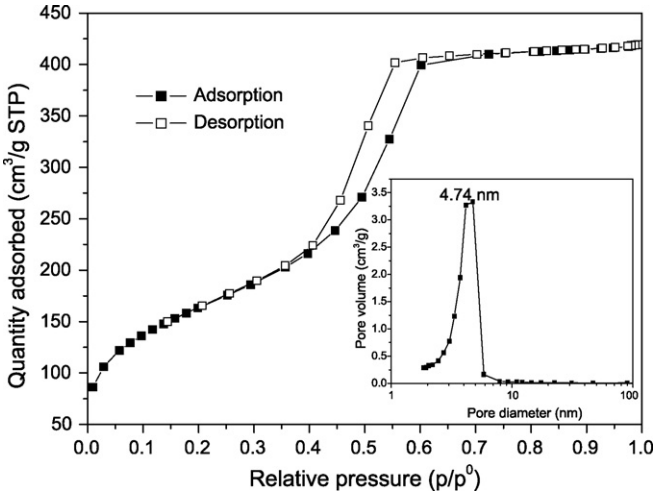

Fig. 3. Nitrogen adsorption/desorption isotherm plots and pore size distribution curve (inset) of SBA-15 sintered at 823 K for 6 h.

pore sizes of the highly porous inner skin-layer (Fig. 1e) and the denser sponge-like outer layer (Fig. 1f), respectively. In contrast with the sponge-like outer layer, the pore volume of the finger-like inner layer is significantly higher, further proving the feasibility of developing a highly compact multifunctional HFMR by depositing catalyst into the finger-like voids through the highly porous inner skin-layer of the substrate.

3.2. Microstructure of the functionalized alumina hollow fibre substrates

Prepared mesoporous SBA-15 yields a type IV isotherm with a H1 hysteresis loop (Fig. 3), which agrees well with a typical adsorption and desorption for mesoporous materials with 2D-hexagonal structures [22]. A well defined step occurs at about $p/p^0 = 0.45–0.55$, associated with the filling of the mesopores as a result of capillary condensation. A narrow pore size distribution (inset of Fig. 3), which was calculated from the adsorption branch based on the BJH model, indicates a uniform pore structure with a mean pore diameter of approximately 4.74 nm, which is consistent with the reported pore sizes of SBA-15 ranging from 4.6 to 30 nm [22]. The BET surface area and the total pore volume of prepared SBA-15 were measured at about 596.58 m^2/g and 0.65 cm^3/g, respectively.

The asymmetric alumina hollow fire substrates were then functionalized by preparing SBA-15 inside the finger-like voids followed by impregnation of Pt. As can be seen in Fig. 4, SBA-15 is success-

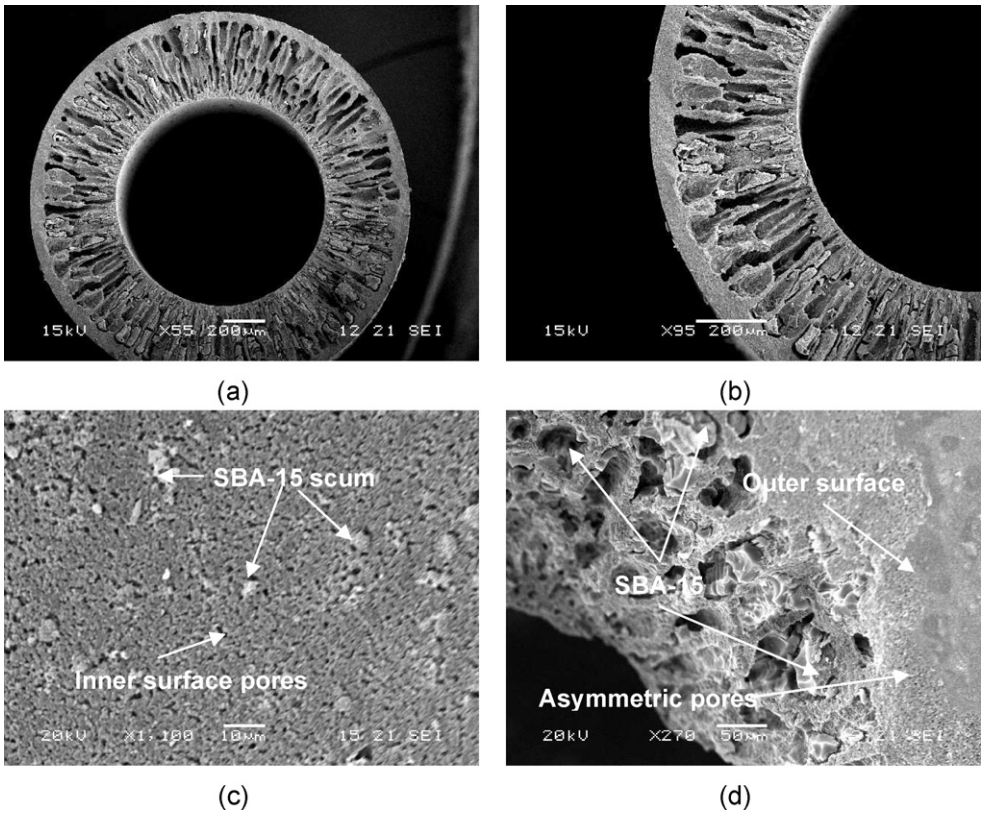

Fig. 4. SEM images of the functionalized alumina hollow fibre substrate: (a) whole view, (b) cross-section, (c) inner surface and (d) top view from outer surface.

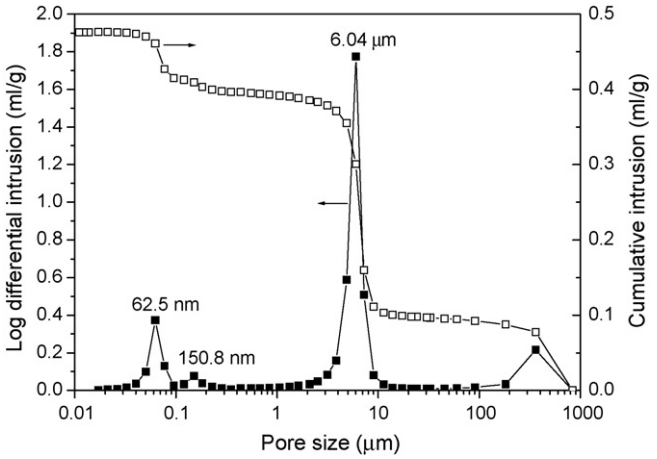

Fig. 5. Mercury intrusion of the functionalized alumina hollow fibre substrates.

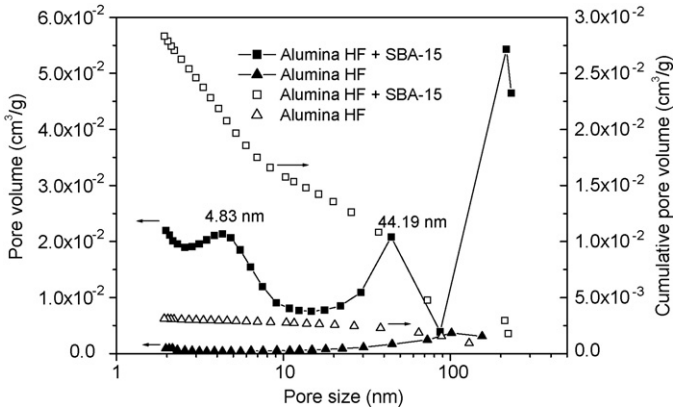

Fig. 6. Pore size (<100 nm) distribution and pore volume of functionalized and untreated alumina hollow fibre substrates.

fully deposited into the alumina hollow fibre substrates (Fig. 4a and b) by using the method described above. Instead of fully blocking the finger-like voids, there is a gap between the deposited SBA-15 and the wall of the finger-like voids after sintering. The pore structures of the inner surface (Fig. 4c) and the outer surface (Fig. 4d) are in good agreement with their untreated counterparts, although a small amount of SBA-15 scum is found scattered loosely across the inner surface. The pore structure of the functionalized substrates, which was further characterized by mercury intrusion and shown in Fig. 5, agrees well with that of the untreated substrates (Fig. 2) except for a new peak at about 62.5 nm, representing one of pore structures in the deposited SBA-15. A comparison between Figs. 2 and 5 further indicates that the deposition of SBA-15 does not significantly change the pore structure of the hollow fibre substrates, because the pore size distribution representing the entrance of the finger-like voids and the one representing the mean pore size of the outer sponge-like layer are consistent with their untreated counterparts. This further suggests that the deposition of SBA-15 does not create significant additional resistance to gas permeation through the functionalized substrates.

The pore structures of the functionalized hollow fibre substrates, especially those less than 100 nm, were characterized by BET. As can be seen in Fig. 6, the peak at 4.83 nm, which represents the mesoporous structure of the deposited SBA-15, agrees well with that in Fig. 3, indicating that the major pore structure of the deposited SBA-15 was confined during the deposition. The peak at 44.19 nm should represent the same pore structure as the one at 62.5 nm in Fig. 5, but differs slightly due to different characterization methods. This indicates that, besides the mesopores in the deposited SBA-15, bigger pores, probably small cracks, were formed during the deposition, which is possibly due to non-uniform shrinking of SBA-15 monoliths in the finger-like voids during the sintering. Furthermore, the functionalized substrates possess a much higher pore volume in contrast with the untreated substrates in view of the pore sizes between 2 and 100 nm, showing the advantages of depositing mesoporous materials of this type into the developed asymmetric hollow fibre substrates in increasing the surface area of the reactor.

The characteristics of the functionalized as well as the untreated substrates are listed in Table 1. In comparison with our previous catalyst deposition method [1], in which sub-micron sized catalyst particles were dispersed in ethanol prior to the deposition, the current method is much more efficient for greater loading of catalyst with a higher surface area, and as a result, yields a significantly higher catalyst surface area in the functionalized substrates. The increase of 5.19 m^2 in the surface area of the reaction zone (5 cm in length) in HFMR-II, which was calculated on the amount of SBA-15 deposited, is much higher than the value of 0.22 m^2 obtained in the previous work for HFMR-I.

3.3. Dehydrogenation of propane to propene

After impregnating Pt into the deposited SBA-15, a multifunctional Pd/alumina HFMR-II was developed by directly coating a Pd membrane of approximately 6 μm in thickness onto the outer surface of the functionalized alumina hollow fibre substrate, using a conventional ELP method [7]. No mechanically weak, intermediate γ-Al_2O_3 layer was employed to modify the substrate surface prior to the coating of the Pd membrane. EDS analysis shown in Fig. 7 reveals that Pd plating solution penetrated slightly into the substrate (approximately 2 μm beneath the substrate surface) during the ELP process, which also agrees with our previous study [1]. The hydrogen permeation flux through the Pd/alumina hollow fibre composite membrane was investigated and described elsewhere [27], because the composite membranes were prepared in the same batch using same preparation conditions.

For comparison, the catalytic activity of the Pt (1 wt.%)/SBA-15 catalyst, which was prepared by a conventional wet impregnation method, was investigated in a fixed bed reactor (FBR) using the same operating conditions as those of the HFMR-II. Approximately 0.1 g of the catalyst was packed into the centre of a dense ceramic tube of 9 mm in diameter. Initial propane conversion values refer to the analysis of the reaction products after 5 min on stream. As can be seen in Fig. 8, the propane conversion started at 75.3% at 773 K and then reduced to 9% after 120 min of the reaction, in agreement with the work of Lobera et al. [29], in which the coke content increased abruptly in approximately the first 10 min, causing rapid catalyst deactivation at the initial stage of the reaction. In the mean time, the propene selectivity increased sharply from 2% to 70% after around 35 min on stream, as a result of deactivation of highly active coor-

Table 1
Characteristics of functionalized and untreated alumina hollow fibre substrates.

	Deposited material	Weight gain (%)	BET S.A. (m^2/g)	Increase of S.A. in reaction zone (5 cm long) (m^2)
Alumina fibre			0.71	
3rd deposition (HFMR-I) [1]	γ-Alumina (180 m^2/g)	0.74	<2.04	0.22
1st deposition (HFMR-II)	SBA-15 (596.58 m^2/g)	6.96	31.83	5.19

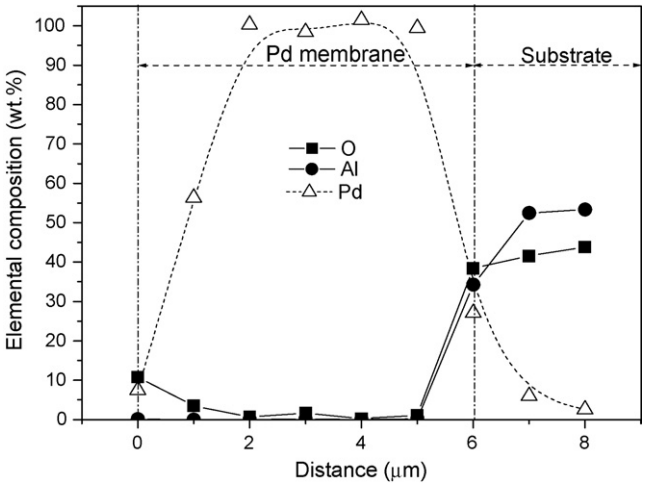

Fig. 7. EDS analysis of the Pd/alumina composite hollow fibre membrane.

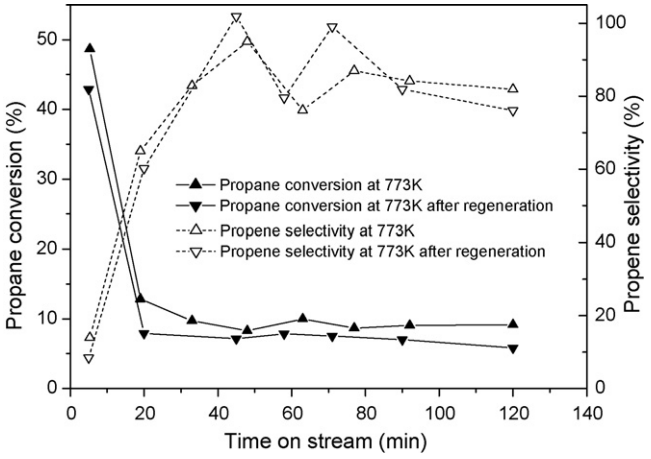

Fig. 9. Dehydrogenation of propane to propene using the multifunctional HFMR-II.

dinatively unsaturated surface Pt sites by coke [23]. This indicates that, although coke-formation is the main reason for catalyst deactivation in the dehydrogenation of propane to propene, the formed coke functioning as a promoter improves the propene selectivity by deactivating the sites that are active for C–C bond activation [23]. Fig. 8 further illustrates that increasing the operating temperature reduces the propane conversion as well as the propene selectivity due to higher level of catalyst deactivation, as a consequence of which the operating temperature of the HFMR-II was chosen to be 773 K.

In contrast with the FBR, the initial propane conversion of the HFMR-II was lower and was measured at approximately 48.7%, as shown in Fig. 9. It has been proved that the use of Pd-based membranes to remove hydrogen as a product from a dehydrogenation reaction enhances the catalyst deactivation in membrane reactors as a consequence of faster coke-formation [4]. As a result, in the first several minutes of the reaction, the propane conversion values in the HFMR-II may be significantly higher than 48.7% and drops sharply before the first product sample in Fig. 9, which was taken 5 min after the reaction, was analyzed. As the reaction proceeds, the propane conversions of the HFMR-II and FBR are comparable. For endothermic dehydrogenation reactions, the high demand for heat means that the products of reaction can be trapped within the pores of the catalyst, resulting in rapid catalyst deactivation due to carbon deposition [4]. Therefore, it is logical to conclude that hydrogen permeation through the membrane is not the rate limiting step, because the rate of hydrogen production in a catalytic membrane reactor of this type is limited by the catalyst productivity [30]. Use of coking-resistant catalysts such as Pt–Sn supported catalysts [31] with high catalytic activity and stability is, in this case, critically important to further improve the performance of membrane reactors of this type. However, the propene selectivity of the HFMR-II is higher than that of the FBR, demonstrating the advantages of the developed HFMR-II in view of the amount of the catalyst employed. After 2 h of testing, the HFMR was regenerated at 773 K overnight, using a stream consisting of 5% of O_2 and 95% of Ar. As can be seen in Fig. 9, the propane conversions after the regeneration were slightly lower than that of the fresh HFMR-II, while the propene selectivity was well recovered.

Although the performance of the FBR and the HFMR-II seem to be comparable in view of the propane conversion and the propene selectivity, much less catalyst is required in the HFMR-II because of the greater surface area of the functionalized alumina hollow fibre substrate. As can be seen in Fig. 10, the volumetric space-time yield (STY) of the HFMR-II is more than 10 times that of the FBR. It should be noted here that this value can be further increased to approximately 20 when smaller ceramic substrates (OD = 1.3 mm) with similar asymmetric structures are employed [28]. In addition, the STY of the HFMR-II, in view of the amount of catalyst employed, is more than 4 times that of the FBR, indicating that the HFMR-II is more efficient in propene production.

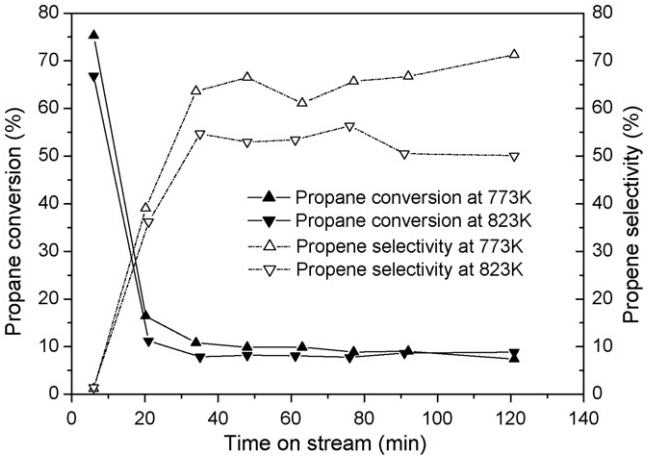

Fig. 8. The catalytic properties of the Pt (1 wt.%)/SBA-15 catalysts in dehydrogenation of propane to propene.

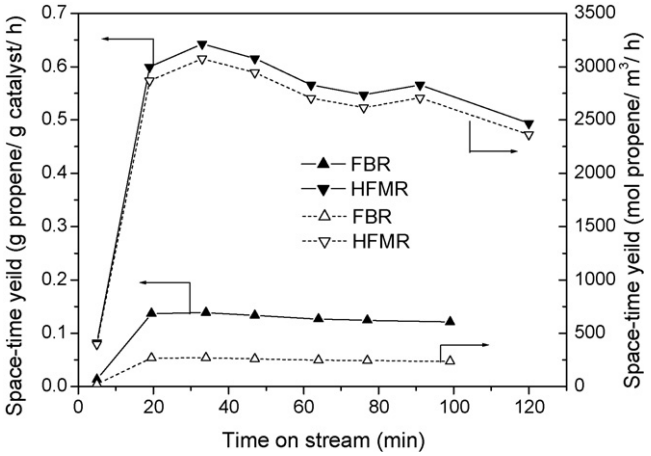

Fig. 10. The space-time yields (STY) the FBR and the HFMR-II.

In comparison with HFMR-I [1], the performances of the two HFMR designs are comparable in regard to propane conversion as well as propene selectivity, which indicates that higher catalyst loading and surface area in the membrane reactor cannot be appreciated as a consequence of fast catalyst deactivation. However, the advantages of the current HFMR design, which have been demonstrated in this study, can be applied to a number of other catalytic reactions of great importance, such as WGS and SR, with less coke-formation problems.

4. Conclusions

Porous alumina hollow fibre substrates with a unique asymmetric pore structure, i.e. a sponge-like outer layer and a finger-like inner layer, and with high surface area/volume ratios of up to 1918.4 m^2/m^3 have been prepared by a one-step dry–wet spinning/sintering method. These substrates are employed to construct a highly compact multifunctional Pd/alumina hollow fibre membrane reactor (HFMR-II) for dehydrogenation of propane. Prior to the direct coating of Pd membranes onto the outer surface of the developed substrates, the substrates were functionalized by depositing mesoporous SBA-15 with a surface area as high as 596.58 m^2/g into the finger-like inner layer, using an easy and efficient method via liquid-paraffin-medium protected solvent evaporation, followed by the impregnation of Pt. This offers both a high catalyst loading and an increase in the surface area of the reaction zone (5 cm in length) in the HFMR-II of 5.19 m^2. Benefiting from this novel design, greater propene selectivity was achieved in the HFMR-II with less catalyst when compared with a conventional fixed bed reactor (FBR) under the same operating conditions, indicating that the developed HFMR-II is more efficient in propene production. The space-time yield (STY) of the HFMR-II was more than 10 times that of the FBR, demonstrating the advantages of the developed HFMR. In comparison with HFMR-I, similar propane conversion as well as propene selectivity was obtained, indicating that higher catalyst loading and surface area in the membrane reactor cannot be appreciated as a consequence of coke-formation. However, the advantages of HFMR-II can be applied to other catalytic reactions with less coking problems, such as the water–gas-shift (WGS) reaction and steam reforming (SR) etc.

Acknowledgments

The authors gratefully acknowledge the research funding provided by EPSRC in the United Kingdom (grant No. EP/F027427/1).

References

[1] Z. Wu, M.I.H. Dzahir, B.F.K. Kingsbury, E. Gbenedio, K. Li, A novel inorganic hollow fibre membrane reactor for catalytic dehydrogenation of propane, AIChE Journal 55 (2009) 2389.
[2] M.V. Mundschau, X. Xie, C.R. Evenson, A.F. Sammells, Dense inorganic membranes for production of hydrogen from methane and coal with carbon dioxide sequestration, Catalysis Today 118 (2006) 12.
[3] Y.S. Lin, Microporous and dense inorganic membranes: current status and prospective, Separation and Purification Technology 25 (2001) 39.
[4] J.N. Armor, Applications of catalytic inorganic membrane reactors to refinery products, Journal of Membrane Science 147 (1998) 217.
[5] J.A. Ritter, A.D. Ebner, State-of-the-art adsorption and membrane separation processes for hydrogen production in the chemical and petrochemical industries, Separation Science and Technology 42 (2007) 1123.
[6] E. Kikuchi, Membrane reactor application to hydrogen production, Catalysis Today 56 (2000) 97.
[7] S.N. Paglieri, J.D. Way, Innovations in palladium membrane research, Separation and Purification Methods 31 (2002) 1.
[8] Y.Y. Liu, X.Y. Tan, K. Li, Mixed conducting ceramics for catalytic membrane processing, Catalysis Reviews: Science and Engineering 48 (2006) 145.
[9] K. Li, Ceramic Membranes for Separation and Reaction, Wiley, 2007.
[10] H. Weyten, J. Luyten, K. Keizer, L. Willems, R. Leysen, Membrane performance: the key issues for dehydrogenation reactions in a catalytic membrane reactor, Catalysis Today 56 (2000) 3.
[11] Y. Yildirim, E. Gobina, R. Hughes, An experimental evaluation of high-temperature composite membrane systems for propane dehydrogenation, Journal of Membrane Science 135 (1997) 107.
[12] X.Y. Tan, S.M. Liu, K. Li, Preparation and characterization of inorganic hollow fiber membranes, Journal of Membrane Science 188 (2001) 87.
[13] X.L. Pan, G.X. Xiong, S.S. Sheng, N. Stroh, H. Brunner, Thin dense Pd membranes supported on alpha-Al_2O_3 hollow fibers, Chemical Communications (2001) 2536.
[14] B.K.R. Nair, J. Choi, M.P. Harold, Electroless plating and permeation features of Pd and Pd/Ag hollow fiber composite membranes, Journal of Membrane Science 288 (2007) 67.
[15] B.K.R. Nair, M.P. Harold, Pd encapsulated and nanopore hollow fiber membranes: synthesis and permeation studies, Journal of Membrane Science 290 (2007) 182.
[16] X.L. Pan, N. Stroh, H. Brunner, G.X. Xiong, S.S. Sheng, Pd/ceramic hollow fibers for H-2 separation, Separation and Purification Technology 32 (2003) 265.
[17] W.P. Wang, S. Thomas, X.L. Zhang, X.L. Pan, W.S. Yang, G.X. Xiong, H-2/N-2 gaseous mixture separation in dense Pd/alpha-Al_2O_3 hollow fiber membranes: experimental and simulation studies, Separation and Purification Technology 52 (2006) 177.
[18] J.H. Tong, L.L. Su, K. Haraya, H. Suda, Thin and defect-free Pd-based composite membrane without any interlayer and substrate penetration by a combined organic and inorganic process, Chemical Communications (2006) 1142.
[19] J.H. Tong, L.L. Su, K. Haraya, H. Suda, Thin Pd membrane on alpha-Al_2O_3 hollow fiber substrate without any interlayer by electroless plating combined with embedding Pd catalyst in polymer template, Journal of Membrane Science 310 (2008) 93.
[20] G.B. Sun, K. Hidajat, S. Kawi, Ultra thin Pd membrane on alpha-Al_2O_3 hollow fiber by electroless plating: high permeance and selectivity, Journal of Membrane Science 284 (2006) 110.
[21] B.F.K. Kingsbury, K. Li, A morphological study of ceramic hollow fibre membranes, Journal of Membrane Science 328 (2009) 134.
[22] D.Y. Zhao, J.L. Feng, Q.S. Huo, N. Melosh, G.H. Fredrickson, B.F. Chmelka, G.D. Stucky, Triblock copolymer syntheses of mesoporous silica with periodic 50 to 300 angstrom pores, Science 279 (1998) 548.
[23] M. Santhosh Kumar, D. Chen, J.C. Walmsley, A. Holmen, Dehydrogenation of propane over Pt-SBA-15: effect of Pt particle size, Catalysis Communications 9 (2008) 747.
[24] P. Shah, V. Ramaswamy, Thermal stability of mesoporous SBA-15 and Sn-SBA-15 molecular sieves: an in situ HTXRD study, Microporous and Mesoporous Materials 114 (2008) 270.
[25] H.F. Yang, Q.H. Shi, B.Z. Tian, S.H. Xie, F.Q. Zhang, Y. Yan, B. Tu, D.Y. Zhao, A fast way for preparing crack-free mesostructured silica monolith, Chemistry of Materials 15 (2003) 536.
[26] Q.Y. Lu, F. Gao, S. Komarneni, T.E. Mallouk, Ordered SBA-15 nanorod arrays inside a porous alumina membrane, Journal of the American Chemical Society 126 (2004) 8650.
[27] M.P. Gimeno, Z.T. Wu, J. Soler, J. Herguido, K. Li, M. Menédez, Combination of a two-zone fluidized bed reactor with a Pd hollow fibre membrane for catalytic alkane dehydrogenation, Chemical Engineering Journal 155 (2009) 298.
[28] C.C. Wei, O.Y. Chen, Y. Liu, K. Li, Ceramic asymmetric hollow fibre membranes—one step fabrication process, Journal of Membrane Science 320 (2008) 191.
[29] M.P. Lobera, C. Téllez, J. Herguido, M. Menéndez, Transient kinetic modelling of propane dehydrogenation over a Pt–Sn–K/Al_2O_3 catalyst, Applied Catalysis A: General 349 (2008) 156.
[30] T. Matsuda, I. Koike, N. Kubo, E. Kikuchi, Dehydrogenation of isobutane to isobutene in a palladium membrane reactor, Applied Catalysis A: General 96 (1993) 3.
[31] S.R. de Miguel, E.L. Jablonski, A.A. Castro, O.A. Scelza, Highly selective and stable multimetallic catalysts for propane dehydrogenation, Journal of Chemical Technology and Biotechnology 75 (2000) 596.